Article:
Hu, K., Reed, D., Robshaw, T.J. et al. (2021) Characterisation of aluminium black dross before and after stepwise salt-phase dissolution in non-aqueous solvents. Journal of Hazardous Materials, 401. 123351. ISSN: 0304-3894

https://doi.org/10.1016/j.jhazmat.2020.123351

Characterisation of aluminium black dross before and after stepwise salt-phase dissolution in non-aqueous solvents

Keting Hu[1], Dan Reed[2], Thomas J. Robshaw[1] Rachel M. Smith[1], Mark D. Ogden[1]

[1]Department of Chemical & Biological Engineering, University of Sheffield, Sheffield, South Yorkshire, S1 3JD, United Kingdom
[2]ALTEK Europe Ltd, Burley Close, Lakeside House, Chesterfield, South Yorkshire, S40 2UB, United Kingdom

Graphical abstract

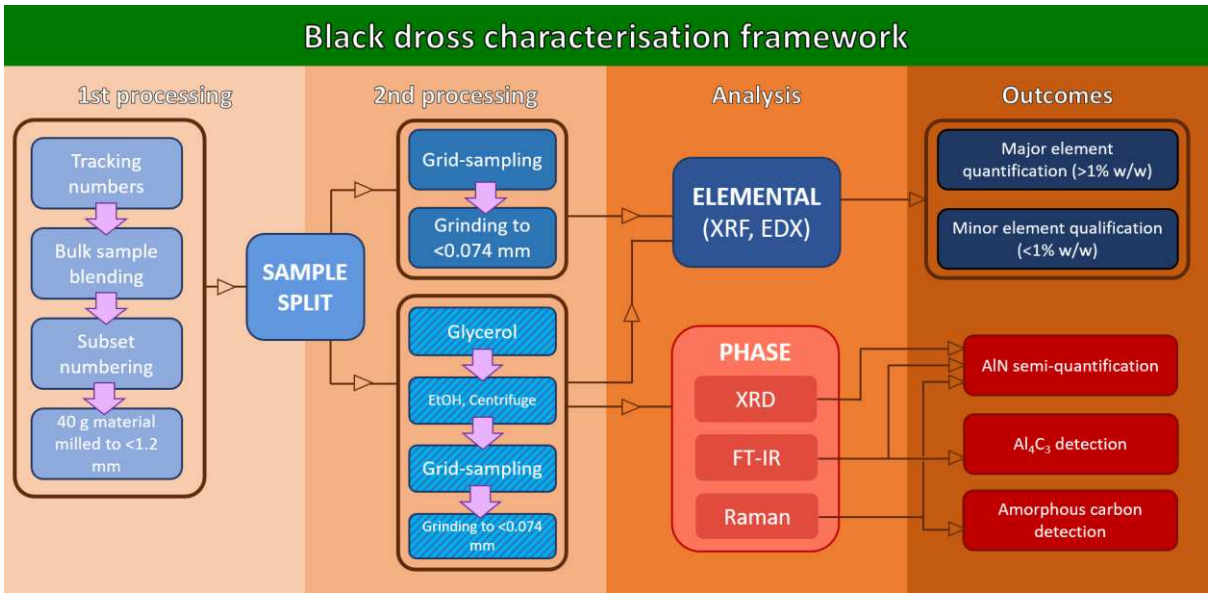

Highlights

• The glycerol pre-treatment method is an effective way to assist in determining minor reactive phases.

• The problematic mineral phases associated with AlN could be easily identified after pre-treatment.

• The existence of amorphous or turbostratic graphitic carbon in black dross has been confirmed.

• The FT-IR allowed the successful identification of Al_4C_3 presence in industrial samples of black dross.

Abstract: Aqueous leaching to recover salts from black dross is accompanied by hazardous gas generation. The gas-generating phases vary significantly across differently sourced black dross. The challenge for industry is how to accurately qualify and quantify the problematic components of black dross, especially minor reactive phases. This paper employed XRF, EDX, XRD, Raman and FTIR to analyse two industrial black dross samples from various sources. A novel pre-treatment method before characterisation was devised using water-free glycerol and anhydrous ethanol to remove the major salt components, without reacting the gas-generating phases. The results show that around 80% of the salts existent in the black dross had been removed successfully through pre-treatment. This method facilitated the determination of minor reactive phases characterised by XRD, XRF and EDX, and had little effect on the characterisation by Raman and FTIR spectroscopy. The ammonia-generating nitride phase was detected by XRD, Raman and FTIR. The FTIR, moreover, allowed the successful identification of carbide. Best practice guidelines for the industrial analysis of black dross has been proposed. The guidelines would provide industry with evidence to include or adjust gas treatment methods and operational parameters when dealing with compositional variability in industrially-sourced black dross.

Keywords: Aluminium black dross, characterisation, hazardous waste, salts dissolution, aluminium nitride

1. Introduction

Due to its unique physical and chemical properties, aluminium (Al) has been widely used in the automobile, aerospace, architectural construction, and marine industries, as well as having many domestic uses [1, 2]. At present, Al is mainly produced via two different routes [3]: primary Al extracted from bauxite ore and secondary Al recycled from scrap and white dross (produced during primary Al production). In the past three decades, approximately 80 million tons of Al has been produced and more than 26 million tons of scrap recycled [4].

In the secondary Al industry, the Al scrap and white dross are re-melted in a furnace with the addition of a large amount of salt flux. The salt flux can effectively help the agglomeration and separation of the molten Al from the solid oxide fraction and protect the metallic Al against oxidation [5]. During the melting process, non-metallic components are absorbed in the liquid flux, forming a by-product referred to as black dross. The black dross is removed by skimming off the top layer of the liquid melt. Depending on the scrap mixture feed, approximately 200-500 kg of black dross is produced per ton of Al [6-8]. In general, black dross contains a large amount of the salt-flux mixture (e.g., NaCl, KCl and fluorides), metal oxide (e.g., Al_2O_3), a small amount of fine metallic Al particles, and some minor contaminants (e.g., Al_4C_3 and AlN) [9].

Black dross has been classified as a hazardous and toxic waste by the EU since 2000 [10] and exposure is considered detrimental to both the environment and human health. Specifically, black dross is considered hazardous with respect to carcinogenicity and skin corrosion/irritation. The non-metallic product (NMP) component of black dross is also a sensitizer and irritant through prolonged or repeated skin or mucous membrane contact [4]. The dust generated from handling black dross is a significant hazard with respect to ingestion and inhalation. In addition, active contaminants in black dross are very sensitive to moisture and react to produce harmful, explosive, poisonous, and unpleasant odorous gases[11, 12]. Potential contaminants AlN, Al_4C_3, AlP, Al_2S_3, and Al_5O_6N present in black dross can

hydrolyse in contact with water producing gaseous ammonia, phosphine, hydrogen sulphide, and methane, in accordance with the following reactions (Equations 1-5) [13-15].

$$AlN_{(s)} + 3H_2O_{(l)} \rightleftharpoons Al(OH)_{3(s)} + NH_{3(g)} \quad \text{(Eqn. 1)}$$

$$2Al_5O_6N_{(s)} + 3H_2O_{(l)} \rightleftharpoons 5Al_2O_{3(s)} + 2NH_{3(g)} \quad \text{(Eqn. 2)}$$

$$AlP_{(s)} + 3H_2O_{(l)} \rightleftharpoons Al(OH)_{3(s)} + PH_{3(g)} \quad \text{(Eqn. 3)}$$

$$Al_2S_{3(s)} + 6H_2O_{(l)} \rightleftharpoons 2Al(OH)_{3(s)} + 3H_2S_{(g)} \quad \text{(Eqn. 4)}$$

$$Al_4C_{3(s)} + 12H_2O_{(l)} \rightleftharpoons 4Al(OH)_{3(s)} + 3CH_{4(g)} \quad \text{(Eqn. 5)}$$

This reactivity means that disposal of this waste material must be strictly controlled and to avoid/minimise environmental pollution, only controlled landfills can be used for the disposal of black dross [16]. Previously, around 95% of the industrially produced black dross was landfilled each year [8]. However, the residual 5% has been steadily accumulating, due to continuing Al production. This current waste stream, including legacy material, needs to be treated urgently, to avoid accidental environmental releases. At present, changing public consciousness and solicitousness regarding the state of the environment is forcing legislators to pass more rigid regulations on pollution. This changing landscape of environmental regulation is also accompanied by a subsequent increase in disposal costs [17]. Consequently the development of a sustainable economic and environmentally-friendly process that can recycle black dross into valuable products is highly sought after by industry [18].

To permit the efficient recovery of the salt flux content of black dross, solubility dictates that an aqueous process is the only sensible option for industrial processing. However, Scharf *et al*. investigated aqueous leaching of black dross, finding that on average, 57 cm^3 of gas was produced per gram of black dross treated [19]. It is imperative that the potential environmental risks of gas emission from dross treatment need to be considered. It would suggest that extensive gas removal would be a pre-requisite for any industrial scale leaching process [20, 21]. The combustible toxic gases produced by aqueous leaching of black dross could be abated in a number of ways: Hydrogen sulphide generated during the process could be oxidised in the dissolution process by addition of hydrogen peroxide [22]. Use of alkaline leaching conditions would lead to the production of ammonia which can be removed by H_2SO_4 / water scrubbers [3]. Phosphine gas produced could potentially be oxidized to produce phosphate fertilizer by a catalytic reaction or absorbed onto activated carbon [3].

Because of the different starting raw materials and metallurgical processes used in secondary Al production, the chemical, mineralogical, and elemental composition of the black dross can vary significantly from source to source [23]. This wide variability in black dross matrix and the potentially different hazardous gases generated would necessitate subsequent adjustments to both gas treatment methods and operational parameters every time an industrial plant dealt with a different type of black dross. To inform changes to industrial processing conditions, it is paramount that the reactive components in each black dross feed be identified. An analytical process that allows the quantitative and qualitative identification of these reactive components in black dross is vital to supporting the development of an economical, sustainable and environmentally friendly process of black dross treatment, which does not rely solely on an expensive controlled landfill option. In previous work, researchers employed XRF and XRD for the chemical and mineralogical analysis which cannot detect all of the harmful components in samples. AlN can only be detected when the content is high (normally over 3%). [4, 24, 25]. So far, there is no literature report that Al_4C_3 in black dross has been identified by XRD . In this paper, samples from two different industrial sources were

investigated by using various solid-state microstructure characterization techniques. Besides XRF and XRD, another three techniques EDX, FTIR and Raman spectroscopy were introduced, to investigate the mineralogy in detail trying to identify more reactive mineral phases. This is the first use of FTIR and Raman in the literature to characterise black dross.

In addition, compared to the large concentration of salts in black dross, the minor toxic gas generating phases are difficult to determine using solid state characterisation methods [3]. We found that the salt phases (such as NaCl, KCl) showed significant solubility in glycerol (the salt phases are about 0.25 times as soluble in glycerol as they are in water) without reacting with the gas evolving species [26]. In this paper, we have developed a novel pre-treatment method to separate the salts from black dross by dissolving them in dry glycerol, without changing the original status of these minor gas generating phases. Since dry glycerol is very viscous and its boiling point is 290 °C [27], it is difficult to remove residual salt-containing glycerol absorbed to the surface of the black dross particles. To solve this issue, anhydrous ethanol was used to wash away residual salt-bearing glycerol from the remaining black dross particles. In this way, the treatment works as a pre-concentration method, where the concentration of non-salt phases in as-received black dross increases. The minor reactive phases can therefore be more readily identified than before pre-treatment. To the best of our knowledge, this pre-treatment of black dross before characterisation has not been reported previously.

Besides, our study, for the first time, has summarised the optimum steps and methods for the characterization of black dross as soon as sample arrives at the plant, accordingly establishing a practical guideline for black dross analysis prior to processing. The establishment of analytical best practice would assist industry in predetermining on plant gas abatement processes and operational parameters. This work is part of an ongoing project to help inform industry with respect to developing an economical and sustainable black dross salt recycling process.

2. Experimental

2.1. Materials

Samples with an average particle size of less than 1.2 mm from two different industrial sources were provided by Altek and designated as A_0 and B_0 in this study. Additionally, the two samples after salt-dissolution treatment were named A_1 and B_1, respectively. All chemical reagents were supplied by Sigma Aldrich at analytical grade or higher, and were used as received. The anhydrous solvents after opening were stored over 5 Å molecular sieves to remove water.

2.2. Salts dissolving tests

In the dissolution tests, 20 g of black dross sample (A_0 or B_0) was added to 400 mL of anhydrous glycerol (40 min contact, 175 rpm agitation, 25 °C). The remaining residual solid was separated by centrifugation (15 min at 4000 rpm). The residual solid (A_1 or B_1) was washed and centrifuged (15 min at 4000 rpm) 3 times with anhydrous ethanol. The solid was then dried in an air-flow oven at 60°C for 24 hours.

A comparison sample was prepared by dissolving 20 g of black dross samples in 400 mL water for 10 minutes (through initial experiments, we observed that, with aqueous treatment,

increasing the contact time further did not result in better leaching) with the same agitation and temperature conditions. The residue was then filtered and dried in an air-flow oven at 60°C for 24 hours.

2.3. Sample preparation and characterisation tests

Before microstructural characterisation by XRF, EDX, XRD and Raman, all samples were ground to fine particles (-0.074mm) using a pestle and mortar. 1 g sample powder was pressed into a tablet (with a diameter of 1.2 cm) using a Powder Tablet Press Machine (Specac Manual Hydraulic Press).

A XRF spectrometer (PANalytical, Zetium model) and a FEG-SEM (FEI NOVA450), equipped with an EDX detector, were employed for elemental quantification. XRF has been done twice and the results were averaged for each sample. The EDX mapping scan has been done twice for each area data collection. XRD data were collected using a Bruker D2 PHASER instrument (Cu K-a radiation, 0.15418 nm). The tube voltage and current, step time, increment and scanning range were 30 kV and 10 mA, 0.4 s, 0.02°, 10°-90° respectively. The powder diffraction file (PDF) patterns database from the International Centre for Diffraction Dara (ICDD) was used for identification and semi-quantification. Raman spectroscopic measurements were carried out using an inVia Raman Microscope, with a laser (514.5 nm, ~2.5 mW) excitation source. The Charge Coupled Device (CCD) exposure time was 20 s and every sample was scanned 2 times. Raman spectral data were generated from 50 cm^{-1} to 4000 cm^{-1}.

FTIR spectroscopy was carried out using a Perkin Elmer Lambda 900 UV/Vis FTIR Spectrophotometer. Samples were prepared for analysis by grinding a known mass of solid with anhydrous Potassium bromide. The sample powder was then pressed at 1000 tons for 1 min and then pressed at 10000 tons for 1 min to produce a pellet for analysis. The wavenumber ranges analysed were from 600 cm^{-1} to 4500 cm^{-1}.

3. Results

3.1. Salt dissolution sample preparation

Water-washing was used to compare the effectiveness of salt-dissolution by glycerol. Table 1 compares the weights of samples obtained before and after sample-washing with dry glycerol and water. All dissolution experiments were conducted at least two times. Errors listed in Table 1 were generated by the standard deviation of duplicate measurements. As shown in Table 1, sample weights obtained after salt-dissolution in glycerol were 11.39g and 13.87g for samples A and B, representing 43.05% and 30.66% weight loss through the pre-treatment process. The corresponding weights of samples A and B, after water-washing were 10.10g and 7.30g respectively, representing 49.50% and 36.50% weight loss for each sample. It can be clearly seen that both samples contained a high concentration of salts and glycerol showed good dissolving ability compared to salts dissolving in water. The large discrepancy in mass-retention between the two samples illustrates the variable composition of black dross, depending on its source.

Table 1. Comparison of sample weights obtained before and after salt-dissolution in glycerol and water (175 rpm agitation, 25 °C)

Sample		Sample A		Sample B	
		A_0	A_1	B_0	B_1
		before salt-dissolution	after salt-dissolution	before salt-dissolution	after salt-dissolution
Glycerol washing (40 min contact)	Mass (g)	20.00±0.01	11.39±0.01	20.01±0.01	13.87±0.01
	Δg (g)	8.61±0.02		6.14±0.02	
	Δg (%)	43.05±2.00		30.66±2.00	
Water washing (10 min contact)	Mass (g)	20.00±0.01	10.10±0.01	20.00±0.01	12.70±0.01
	Δg (g)	9.90±0.02		7.30±0.02	
	Δg (%)	49.50±2.00		36.50±2.00	

3.2. XRF analysis

The chemical compositions of the two sourced samples, before and after pre-treatment, were identified using XRF (Fig. 1), and the specific values are listed in Table S1 in the supplemental materials. Overall, all samples had complex chemical constituents, with 27 and 29 elements detected in sample A and B, respectively. Specifically, 26 elements were found in A_0, 23 in A_1, 28 in B_0 and 26 in B_1. The content of Na, Mg, Al, Si, Cl, K and Ca were all over 1% by weight (Fig. 1-(a) and (c)). These elements were treated as major elements in black dross samples. Comparatively, P, S, Ti, V, Cr, Mn, Fe, Co, Ni, Cu, Zn, Ga, Se, Br, Sr, Zr, Mo, Rh, Cs, Ba, Ce, Pb, Bi were minor constituents (Fig 1-(b) and (d)). The two different industrially sourced samples A and B all contained the same types of major elements. However, some of the minor elements were not included in both samples. For example, sample A did not contain Se, Cs and Ce, while Mo did not exist in sample B.

Fig. 1-(a) and (c) obviously show that after pre-treatment, the salt content Na, K and Cl has been largely decreased (elements are circled in red). In contrast, due to the dissolution of salts from the original samples, the amount of other major elements, (such as Mg, Al, Si, Ca) relatively increased substantially. Obviously, pre-treatment facilitates the observation of these major elements. However, as shown in Fig. 1-(b) and (d), the increasing trends for minor elements after pre-treatment of dissolving salt-phases were not obvious. The reason for this was the minor element amounts after pre-treatments were still too low to be easily detected by XRF due to its resolution.

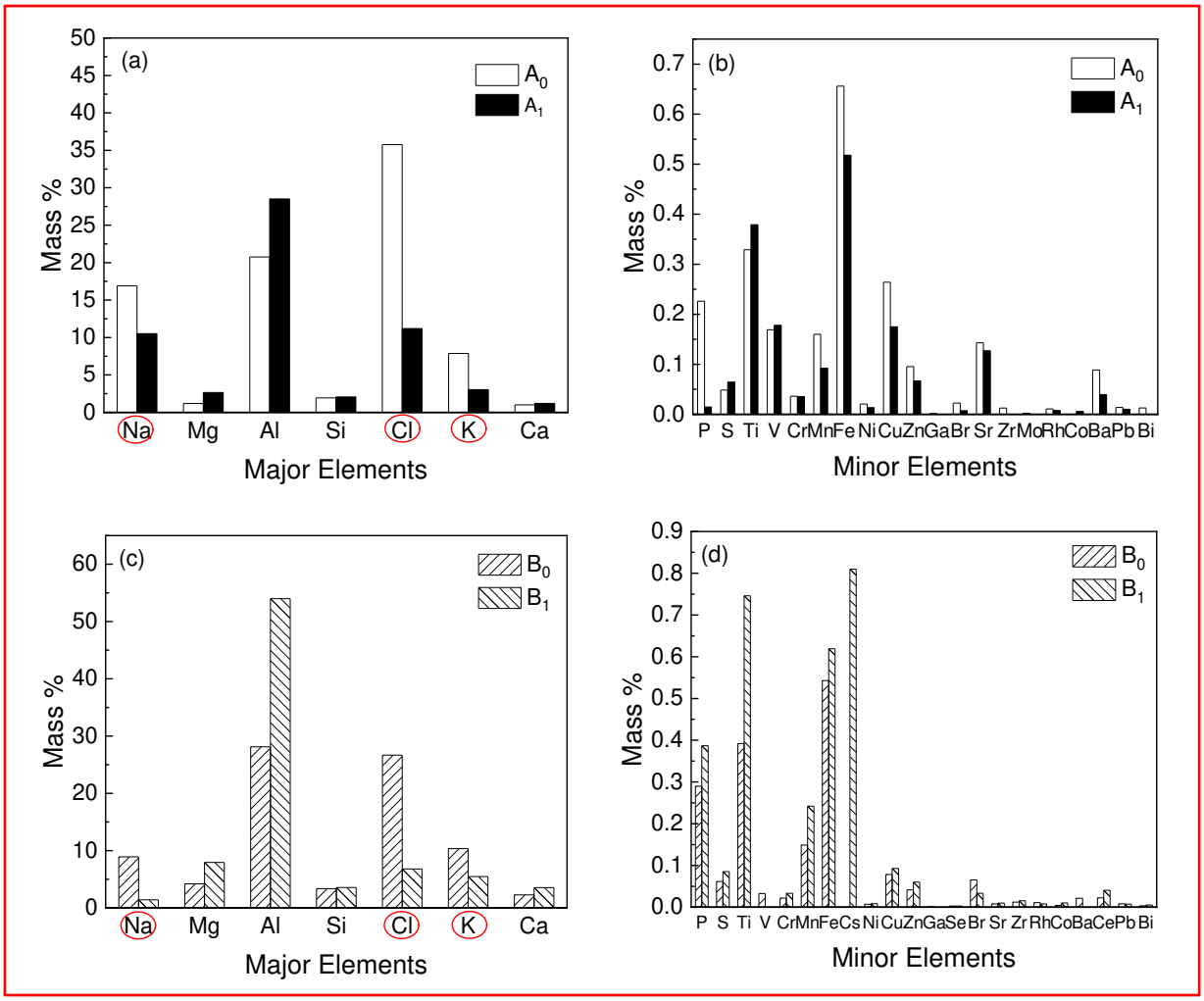

Fig. 1. Chemical analysis of aluminium black dross from two different sources before (A_0, B_0) and after (A_1, B_1) salt-phases dissolution in glycerol and ethanol by XRF-(a) and (c) Elements with weight content over 1%; (b) and (d) Elements with weight content below 1%

3.2. EDX elemental quantification

The chemical compositions of two samples before and after pre-treatment were investigated by EDX mapping from various areas of the samples. Each sample was scanned at least 5 different areas, over its whole surface area. The average elemental quantification is shown in Fig.2. It is seen that elements O, Al, Cl, N, Na, K, Mg, Si, Ca, Fe, Ti, Mn, Zn, S, Mo, and Nd were detected in both samples. F, Cu, V, Yb, Ba, and Ni were discovered in sample A, while P, Cr and Eu were only observed in sample B. More specifically, there were 18 elements in A_0, 18 elements in A_1, 18 in B_0, and 14 in B_1 with different minor elements. Compared to XRF results, N, O, F, P and Eu were detected by EDX only. It is obvious that both samples from various sources contained a large number of elements, and showed species variability in the minor contaminant or alloying elements.

The change in concentrations of elements, shown in EDX analysis, before and after salt-dissolution, was similar to the XRF results. It is clear that the concentrations of elements Cl, Na, K, which majorly contributed to salt phases, were decreased in both samples after pre-treatment. It is noticeable that the problematic element N, which contributes to the formation of nitrides was detected in sample A_1 (circled in red in Fig. 2) after salt-dissolution, yet was not found in sample A_0. Also, after multiple scans, the detection frequency of element N was

higher in the sample B_1 after salt-dissolution. The specific data obtained from multiple scans can be found in Figure S1 in the supplemental materials.

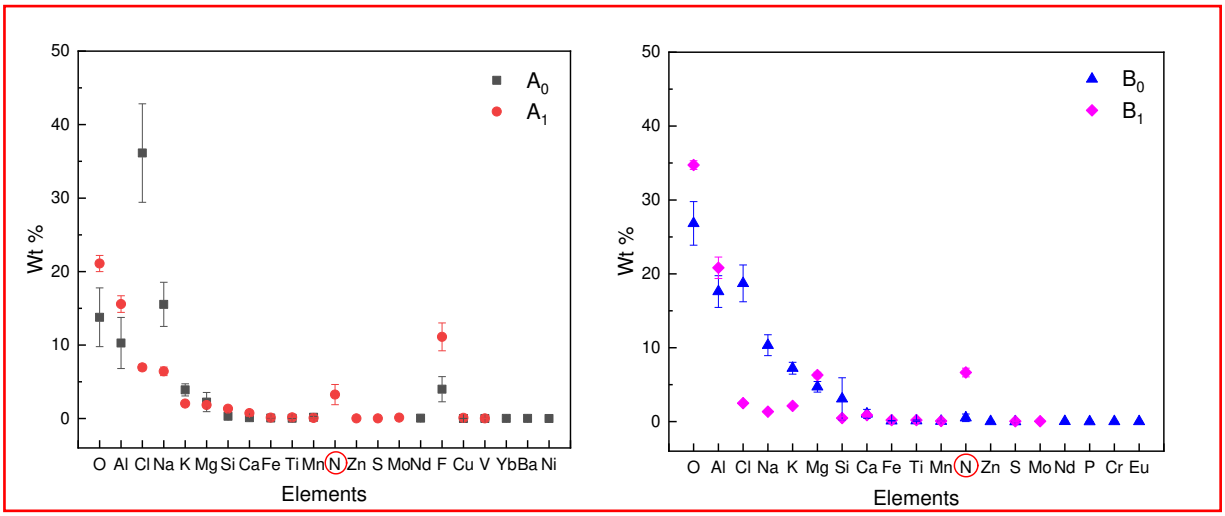

Fig. 2. Chemical analysis of aluminium black dross from two different sources before (A_0, B_0) and after (A_1, B_1) salt-phases dissolution in glycerol by EDX

3.3. XRD analysis

The XRD patterns before and after salt-dissolution in glycerol are shown in Fig. 3. Subsequent to salt-dissolution, the intensity of a number of inorganic salt peaks for both samples was significantly reduced. In contrast, characteristic peaks of other phases have been largely magnified and much more obvious. Though some published work has reported that AlN is a major phase in black dross[4], the amount was usually too low to be detected compared to the huge amount of other salts present. From Fig. 3, it can be seen that for sample A_0, AlN was not detected (no peaks observed at 2theta values of 33.226, 36.056, 37.943, 49.838, 59.367, 66.077). However, after salt-dissolution, it could be detected and analysed easily (sample A_1). From the XRD results of sample B_0 and B_1, the characteristic peaks of AlN were magnified in B_1 compared to the sample B_0. The values of AlN, semi-quantified by XRD are listed in Table. 2. The pre-treatment method enabled XRD to detect those minor and problematic phases existing in residual black dross more easily than in original samples. This result was highly consistent with the results of N content in the various samples detected by EDX (Fig. 2).

Table 2 The content of AlN in the samples from two sources before (A_0, B_0) and after pre-treatment (A_1, B_1)

	A_0	A_1	B_0	B_1
AlN content (%)	ND*	3	4	9

* not detectable.

Furthermore, halite (NaCl), corundum (Al_2O_3), aluminium nitride (AlN), sylvite (KCl), spinel ($MgAl_2O_4$), and quartz (SiO_2) could be identified in both samples A and B. cryolite (Na_3AlF_6) was found in A_0 and A_1, while Fluorite (CaF_2) was observed in B_0 and B_1. An extra phase Diaoyudaoite ($NaAl_{11}O_{17}$) could only be detected in sample A_1. However, the XRD analysis results did not contain all the elements detected by XRF and EDX results. The reason for this is that the concentrations of other phases containing those elements were below the XRD detection limit.

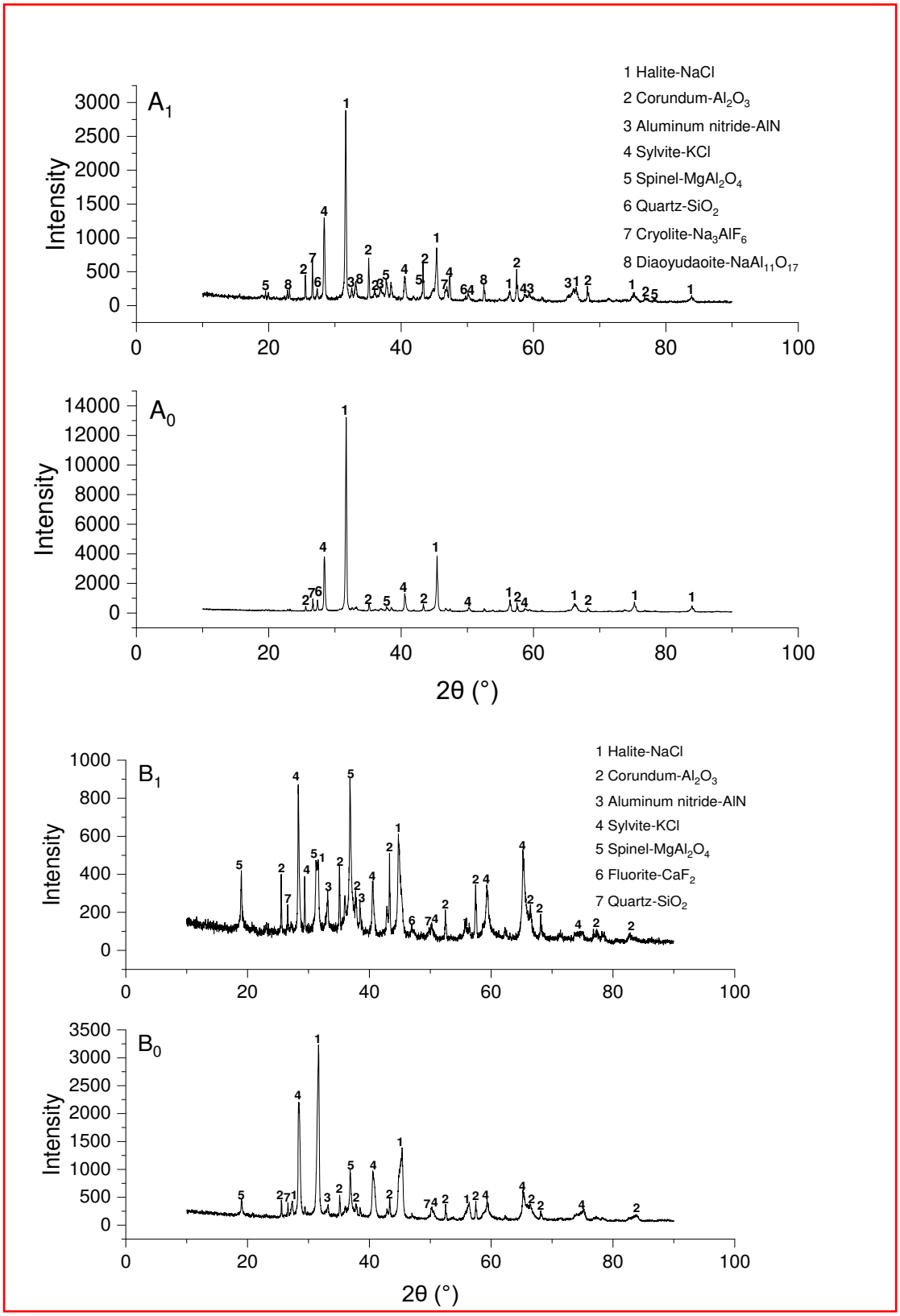

Fig. 3. Mineralogical phases of aluminium black dross from two different sources before (A_0, B_0) and after (A_1, B_1) salt-phase dissolution in anhydrous glycerol and ethanol

3.4. Raman spectra

Many mineral-phases contained in black dross are Raman active. It should be noted that the locations of the peaks were not the same for each curve. Because for heterogeneous samples, the species abundance in the area of the sample illuminated by the laser spot could not represent the entire sample, characteristic spectra from some minor mineral phases could only be identified in some of the scans. Therefore, at least 10 Raman spectra have been done for an accurate representation of bulk samples. Fig. 4 shows representative Raman spectra for each sample before (A_0, B_0) and after (A_1, B_1) salt-phases dissolution. The Second Derivative method was used to correct the baselines, using OriginPro software.

Based on the Raman spectrum of AlN reported previously [28], the dominant Raman scattering peak was located at ~658 cm^{-1}. It could therefore be ascertained that AlN was contained in sample A_0 (Fig. 4). In addition, the huge peaks around 1340 cm^{-1} and 1600 cm^{-1} that were observed in all of the samples, corresponding to the D and G band regions of carbon, indicated the existence of amorphous or turbostratic graphitic carbon in the samples [29].

After salt-dissolution, no new characteristic phase peaks were observed compared to the species detected before pre-treatment.

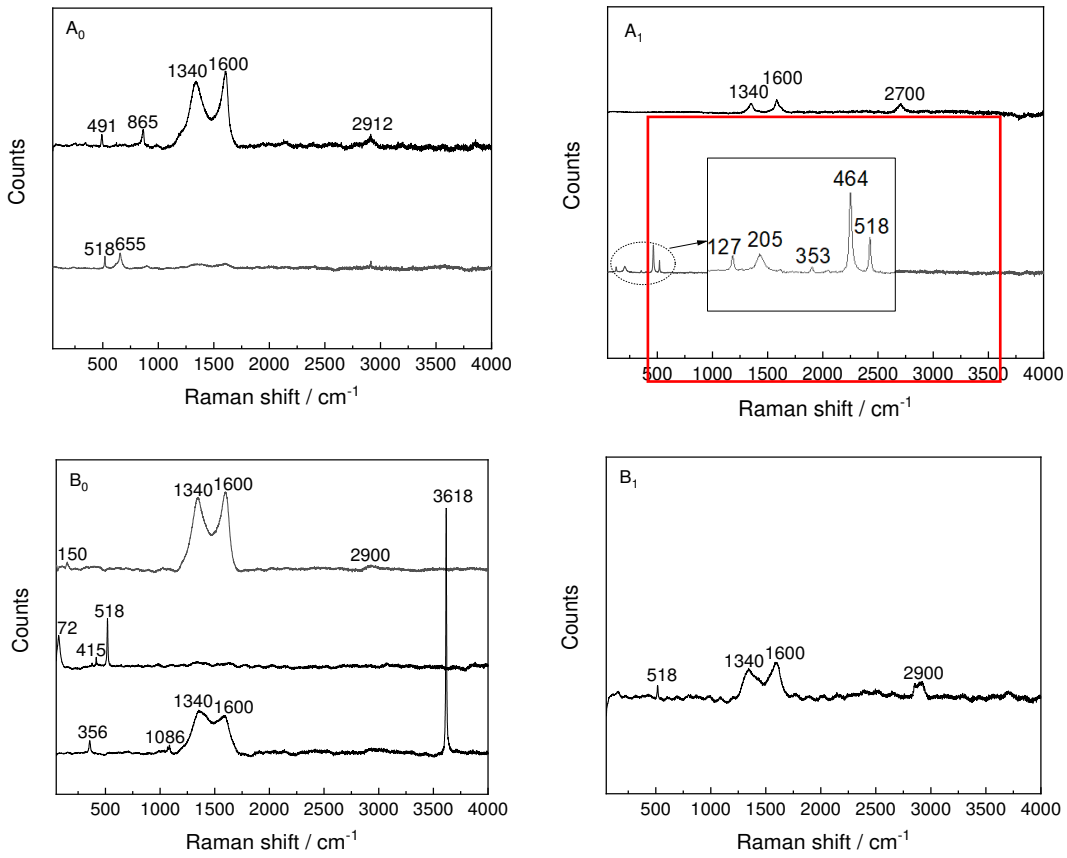

Fig. 4. Raman analysis of aluminium black dross from two different sources before (A_0, B_0) and after (A_1, B_1) salt-phases dissolution in glycerol and ethanol. Multiple spectral lines in the same graph represent different analysis points from the same sample.

3.5. FTIR spectra

Fig. 5 illustrates the FTIR spectra of the two different samples before (A_0, B_0) and after (A_1, B_1) salt-dissolution. It can be observed that the spectra of samples before and after salt-dissolution are similar for the two sourced samples. Thus, the pre-treatment has little effect on FTIR characterisation.

According to the spectral repository "SpectraBase" [30], aluminium carbide characteristic peaks would be expected at around 700 and 640 cm^{-1}, which matched perfectly with the FTIR spectra of sample A, indicating the existence of Al_4C_3. This is the first direct identification of the existence of aluminium carbide in black dross, using FTIR spectroscopy. Previous identification methods[31] were inferred indirectly from carbon content assays. It is clear that this previous method can only estimate the existence of Al_4C_3 in black dross, which is inaccurate. The reason for this is evidenced in our study by the Raman spectra, showing obvious characteristic peaks for amorphous or turbostratic graphitic carbon in sample A. Also, as shown in Raman data, sample B still contained carbon. Yet, the FTIR spectra did not show obvious characteristic peaks of Al_4C_3, which indicated that the Al_4C_3 content in sample B was much lower than sample A.

It is reported that AlN has a dominant characteristic FTIR peak range from 600-1000 cm^{-1} [32]. As shown in Fig. 5, the AlN phase could be confirmed again in sample B by FTIR.

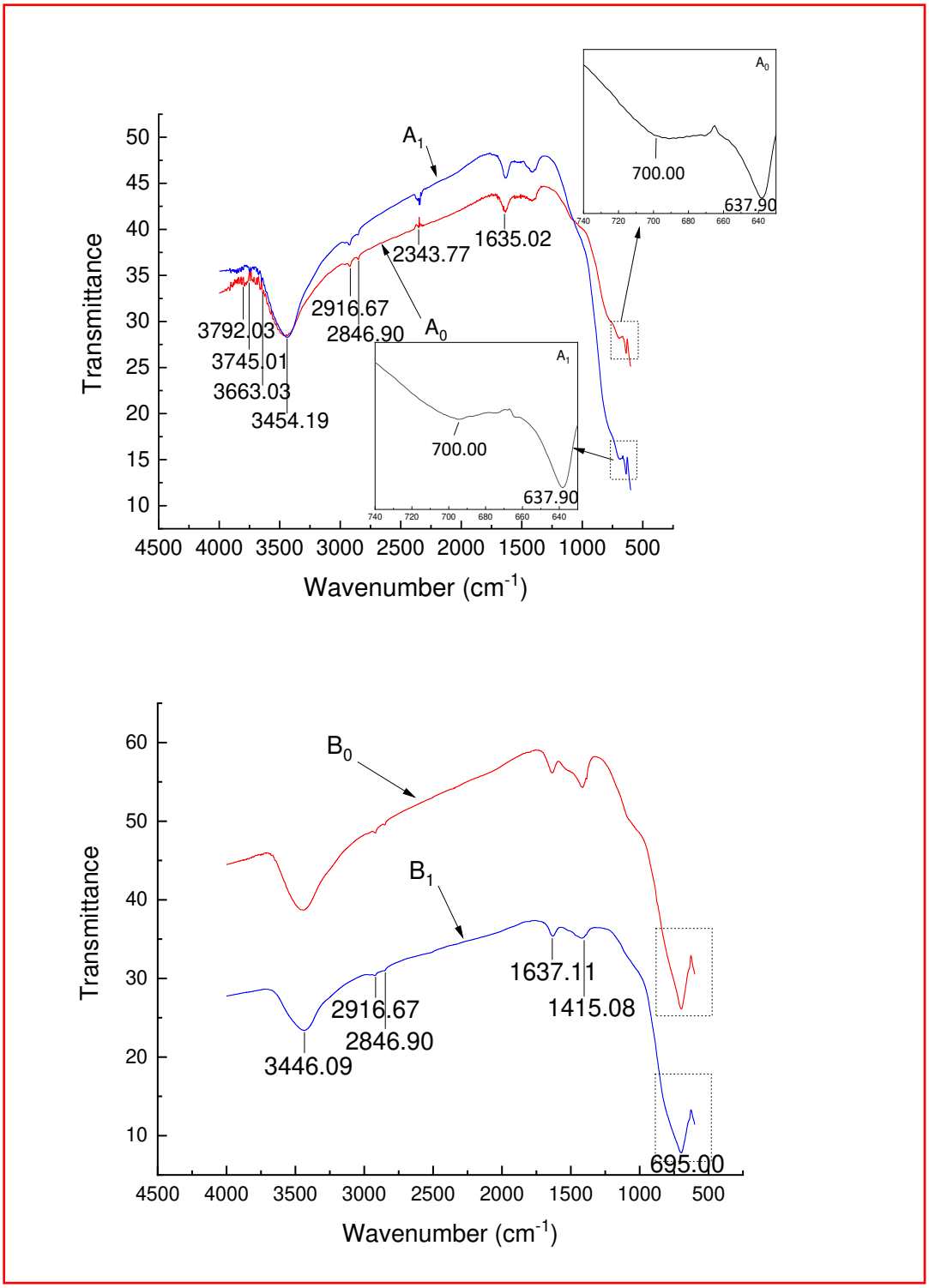

Fig. 5. FTIR analysis of aluminium black dross from two different sources before (A_0, B_0) and after (A_1, B_1) salt-dissolution in glycerol and ethanol

4. Discussion

4.1 Improving the industrial characterisation of black dross

A best practice guideline for industrial analysis of black dross is given in Fig. 6. The samples were blended, labelled and collected upon arrival at the processing plant. Each sample was divided into two parts for characterisation preparation: one was directly subjected to

preparation, and the other one was processed with further pre-treatment. After that, various characterisation methods were used for analysis.

In general, it is widely reported that black dross usually contains 40-55% salt-flux mixture [8]. From our proposed salt-dissolution sample preparation methodology, an observable weight loss of 43.05% and 30.66% from sample A and B respectively was observed. This infers that a single sample treatment removes approximately 80% of the salt present in the black dross sample. This subsequent treatment of glycerol dissolution and ethanol washing leads to a pre-concentration of non-salt phases by approximately 1.6 and 1.8 times in sample A and B. This means that more minor phases within the original black dross sample below the detection limit of different characterisation techniques can exceed the detection limit after this pre-treatment process. In the future, the salt could potentially be recovered from the glycerol by solvent evaporation or crystallization, by tuning solvent polarity, but this is currently beyond the scope of this paper, which is focused upon problematic species identification. Thus, the salt glycerol phase was not studied further.

In this study, the elemental distribution in two sourced samples was characterised by XRF and EDX. A side-by-side comparison of the elements detected by these two techniques is shown in Table S2. Obviously, the main difference of elements distributed in various sources was the existence of different minor alloying elements. Of these, some were detectable only by XRF (Co, Ga, Br, Sr, Zr, Rh, Cs, Ce, Pb, Bi) and some only by EDX (Nd, Yb, Ba Eu). The instrument favoured by a particular plant would probably be dictated by economics and by the level of interest and feasibility in recovering and reprocessing elements of potential value.

Based on phase analysis results, pre-treatment by dissolving salt phases in glycerol and ethanol was beneficial, in allowing for characterisation of reactive phases present in black dross. XRD data could reflect more accurately AlN figures, while FTIR allowed the detection of Al_4C_3. In addition, amorphous carbon could be identified by Raman.

It can be seen that following the guidelines in Fig.6, more detailed components of black dross could be identified clearly to inform plant treatment processes.

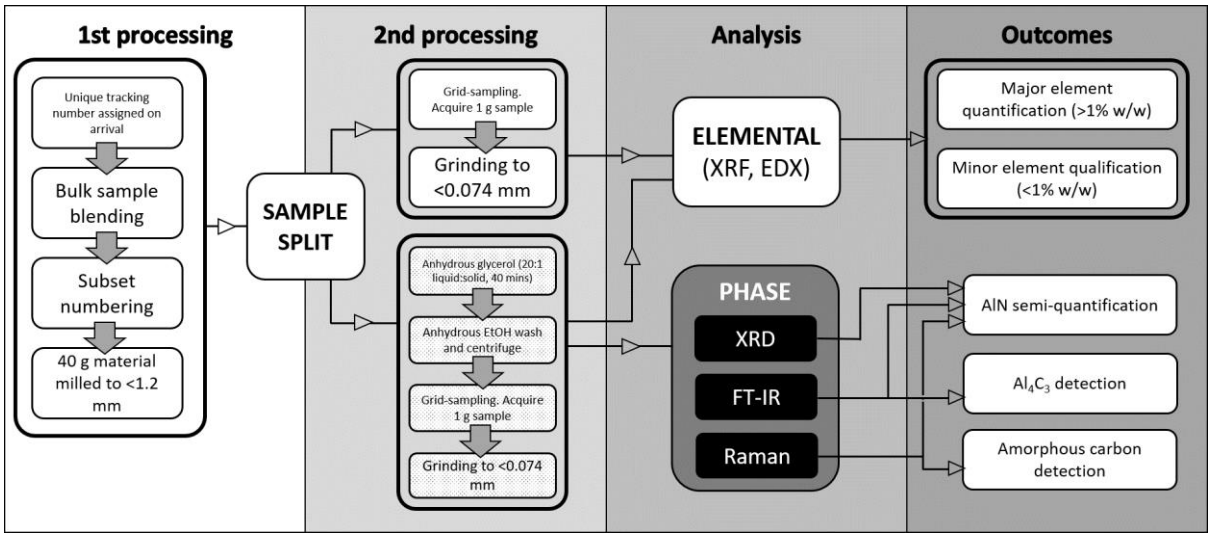

Fig. 6 A guideline of black dross analysis in the industry

4.2 The effect of feed variability on the characterisation and salt recycling process

In this study, more than 8 phases and nearly 30 elements have been identified in black dross. The various constituents can be attributed to a great variety of alloying elements existing in Al scraps and the differences in operating practices when various Al alloys are produced [3, 23, 33]. Specifically, NaCl, KCl and CaF_2 originated from the molten salt flux, which is commonly used during the melting process. The corundum came from the reaction of the atmospheric oxygen with molten metallic aluminium at high temperatures. $MgAl_2O_4$ was the result of oxidation of Mg present in the Al scrap as an alloying element during melting. As reported [4], black dross may also contain $CaCO_3$ which was not detected in our study. This could be attributed to the partial carbonization of portlandite $Ca(OH)_2$, previously formed during hydration of CaO.

Not all the contamination phases, such as nitrides, carbides, phosphide and sulphide, could be readily detected. AlN can be easily formed, due to the negative Gibbs energy below 283.6 K of the reaction between molten Al and atmospheric nitrogen, occurring after the removal of black dross from the melting furnace [34-36]. Al_4C_3 is formed when molten Al reacts with dispersed carbon particles. These are introduced from scraps such as paints and plastic coatings on Al cans and absorbed by the salt slag during the melting process [3, 21]. Aluminium phosphide and sulphide, which have not been found in our study, could be formed through the reaction of Al with phosphates and sulphates in the feed [3, 37].

Black dross is not only complicated, but also diverse in nature, according to site of origin. It is reported that the variability of mineral composition exists not only across plants, but within samples from the same plant as well [7]. Here we only focus on the range of contaminating phases. Huang [7] investigated 39 samples from 10 different plants, which showed that the average content of AlN contained in the sample was 4.6%, (range: 0-10%). Other work [9, 20, 34, 37-42] has reported that salt cake from secondary Al processing can contain 0-30% Al. Xiao et al.[21] has reported that typical salt slag contains: 1% AlN, 7-8% Al_4C_3, and about 0.1% AlP.

For the salt-recycling process, the feed variability determines the different methods and operational parameters for toxic contaminant treatment during processing. Some sources of black dross contain a high amount of nitride, while others contain carbides. This requires industry to add abatement methods for the generated gases, since the possible generated gases (Equations 1-5) ammonia, phosphine and hydrogen disulfide are highly toxic. Methane is flammable and a more potent greenhouse gas than CO_2. As our results show (Figs.1-5), the problematic phases were AlN in both samples, and Al_4C_3 in sample A. Although AlN was not detected in sample A_0 before pre-treatment, 3% AlN was detected after salt-dissolution using the pre-treatment process. For sample B, 4% and 10% AlN were determined before and after pre-treatment. Considering possible treatment methods, H_2SO_4 / water scrubbers should be added to treat ammonia generated from AlN during industrial processing for sample A and B. In the leaching of sample A, methane produced from Al_4C_3 could be valorised by burning to use the thermal energy.

Clearly, detailed information of samples acquired by using multiple-scale characterisation methods is key to facilitate the industry to set up appropriate operating parameters and control the hazardous gas generation (Fig. 6). It can also reduce unnecessary processing setup costs in the industrial salt-leaching recovery process as well.

5. Conclusions

Aluminium black dross is a very complex mixture consisting of salts, various metal oxides and a plethora of reactive phases. Moreover, the phases and corresponding volume fractions vary significantly with different industrial and recycled aluminium feed sources. In industry, different toxic gas treatment methods involving aqueous leaching are normally used for recycling salts. A new pre-treatment is presented in this paper, which dissolves the major salt-phases in black dross with glycerol and ethanol. It is seen to be an effective way to assist in determining minor phases.

In this study, samples A and B from two different industrial sources contained 36 elements in total. Na, Mg, Al, Si, P, S, Cl, K, Ca, Ti, V, Cr, Mn, Fe, Co, Ni, Cu, Zn, Ga, Br, Sr, Zr, Mo, Rh, Pb, Bi, N, O, Nd were detected in both samples. However, F, Yb, Ba, were only discovered in sample A, while Eu, Se, Cs, and Ce were only observed in sample B. The mineral phases of halite (NaCl), corundum (Al_2O_3), sylvite (KCl), spinel ($MgAl_2O_4$), quartz (SiO_2), fluorite (CaF_2), cryolite (Na_3AlF_6) and Diaoyudaoite ($NaAl_{11}O_{17}$) were identified. The existence of amorphous or turbostratic graphitic carbon has been confirmed by Raman spectroscopy. The toxic phase AlN has been identified by XRD, Raman and FTIR. One of the other gas generating phases Al_4C_3 has been, for the first time, detected using FTIR.

Both the pre-treatment methodology and proposed framework for sample-processing could help in the future remediation and valorisation of black dross waste.

Credit Author Statement

KH, DR, and MO conceived and designed the study. KH performed the experiments and analysed the data. KH, DR, RS, MO and TR discussed the data. KH and MO drafted the manuscript. KH, MO and TR revised the manuscript. All co-authors approved the final submitted version of the manuscript.

Declaration of interests

The authors declare that they have no known competing for financial interests or personal relationships that could have appeared to influence the work reported in this paper.

Acknowledgements

This work was supported by Innovate UK funding through Knowledge Transfer Partnership (KTP010597) with Altek Europe Ltd on developing black dross treatment processing methods. The authors would like to thank the members of the Separations and Nuclear Chemical Engineering Research (SNUCER) group at the University of Sheffield who offered help and support with this work. Thank you to lab staff at the University of Sheffield for offering assistance in facility use.

References

[1] D. Brough, H. Jouhara, The aluminium industry: A review on state-of-the-art technologies, environmental impacts and possibilities for waste heat recovery, International Journal of Thermofluids, 1-2 (2020) 100007.

[2] P. Garg, A. Jamwal, D. Kumar, K.K. Sadasivuni, C.M. Hussain, P. Gupta, Advance research progresses in aluminium matrix composites: manufacturing & applications, Journal of Materials Research and Technology, 8 (2019) 4924-4939.

[3] M. Mahinroosta, A. Allahverdi, Hazardous aluminum dross characterization and recycling strategies: A critical review, Journal of Environmental Management, 223 (2018) 452-468.

[4] P.E. Tsakiridis, P. Oustadakis, S. Agatzini-Leonardou, Aluminium recovery during black dross hydrothermal treatment, Journal of Environmental Chemical Engineering, 1 (2013) 23-32.

[5] O. Majidi, S.G. Shabestari, M.R. Aboutalebi, Study of fluxing temperature in molten aluminum refining process, Journal of Materials Processing Technology, 182 (2007) 450-455.

[6] Y. Seng, W. Z. Cheng, Y. G. Qun, Treatment of the aluminum waste residus and waster ashes [J], Non-ferrous Metals Recycling and Utilization, 10 (2006) 22-24.

[7] X.L. Huang, A.E. Badawy, M. Arambewela, R. Ford, M. Barlaz, T. Tolaymat, Characterization of salt cake from secondary aluminum production, Journal of Hazardous Materials, 273 (2014) 192-199.

[8] P.E. Tsakiridis, Aluminium salt slag characterization and utilization – A review, Journal of Hazardous Materials, 217-218 (2012) 1-10.

[9] H.N. Yoshimura, A.P. Abreu, A.L. Molisani, A.C. Camargo, J.C.S. Portela, N.E. Narita, Evaluation of aluminum dross waste as raw material for refractories, Ceramics International, 34 (2008) 581-591.

[10] C. European, Commission decision of 3 May 2000 replacing decision 94/3/EC establishing a list of wastes pursuant to article 1(a) of council directive 75/442/EEC on waste and council decision 94/904/EC establishing a list of hazardous waste pursuant to Article 1(4) of council directive 91/689/EEC on hazardous waste, Official Journal European Community, (2000) 3-24.

[11] C. European, Commission decision of 16 November 2000 defining the specifications of projects of common interest identified in the sector of the trans-European energy networks by Decision No 1254/96/EC of the European Parliament and of the Council, Official Journal of the European Communities, L305 (2000) 22-31.

[12] G.V. Calder, D. Stark Timothy, Aluminum Reactions and Problems in Municipal Solid Waste Landfills, Practice Periodical of Hazardous, Toxic, and Radioactive Waste Management, 14 (2010) 258-265.

[13] N.W. Liu, M.S. Chou, Reduction of secondary aluminum dross by a waste pickling liquor containing ferrous chloride, Sustainable Environment Research, 23 (2013) 61-67.

[14] A. Abdulkadir, A. Ajayi, M.I. Hassan, Evaluating the Chemical Composition and the Molar Heat Capacities of a white Aluminum Dross, Energy Procedia, 75 (2015) 2099-2105.

[15] R. Galindo, I. Padilla, O. Rodríguez, R. S. Hernández, S. L. Andrés, A. L. Delgado, Characterization of solid wastes from aluminum tertiary sector: The current state of Spanish industry, Journal of Minerals and Materials Characterization and Engineering, 3 (2015) 55-64.

[16] M. Hanifzadeh, Z. Nabati, P. Longka, P. Malakul, D. Apul, D.S. Kim, Life cycle assessment of superheated steam drying technology as a novel cow manure management method, Journal of Environmental Management, 199 (2017) 83-90.

[17] A. Gil, S.A. Korili, Management and valorization of aluminum saline slags: Current status and future trends, Chemical Engineering Journal, 289 (2016) 74-84.

[18] N. Murayama, I. Maekawa, H. Ushiro, T. Miyoshi, J. Shibata, M. Valix, Synthesis of various layered double hydroxides using aluminum dross generated in aluminum recycling process, International Journal of Mineral Processing, 110-111 (2012) 46-52.

[19] C. Scharf, A. Ditze, Recycling of black dross containing rare earths originating from melting and recycling of magnesium alloys, Hydrometallurgy, 157 (2015) 140-148.

[20] B. Lucheva, T. Tsonev, R. Petkov, Non-waste aluminium dross recycling, Journal of the University of Chemical Technology and Metallurgy, 40 (2005) 335-338.

[21] Y. Xiao, M.A. Reuter, U.D.O. Boin, Aluminium Recycling and Environmental Issues of Salt Slag Treatment, Journal of Environmental Science and Health, Part A, 40 (2005) 1861-1875.

[22] A. Couvert, I. Charron, A. Laplanche, C. Renner, L. Patria, B. Requieme, Treatment of odorous sulphur compounds by chemical scrubbing with hydrogen peroxide-Application to a laboratory plant, Chemical Engineering Science, 61 (2006) 7240-7248.

[23] B.R. Das, B. Dash, B.C. Tripathy, I.N. Bhattacharya, S.C. Das, Production of η-alumina from waste aluminium dross, Minerals Engineering, 20 (2007) 252-258.

[24] A.K. Tripathy, S. Mahalik, C.K. Sarangi, B.C. Tripathy, K. Sanjay, I.N. Bhattacharya, A pyro-hydrometallurgical process for the recovery of alumina from waste aluminium dross, Minerals Engineering, 137 (2019) 181-186.

[25] Q. Yang, Q. Li, G. Zhang, Q. Shi, H. Feng, Investigation of leaching kinetics of aluminum extraction from secondary aluminum dross with use of hydrochloric acid, Hydrometallurgy, 187 (2019) 158-167.

[26] S.P. Pinho, E.A. Macedo, Solubility of NaCl, NaBr, and KCl in Water, Methanol, Ethanol, and Their Mixed Solvents, Journal of Chemical & Engineering Data, 50 (2005) 29-32.

[27] R. Christoph, B. Schmidt, U. Steinberner, W. Dilla, R. Karinen, Glycerol, Ullmann's Encyclopedia of Industrial Chemistry.

[28] X. Li, C. Zhou, G. Jiang, J. You, Raman analysis of aluminum nitride at high temperature, Materials Characterization, 57 (2006) 105-110.

[29] F.S. Sayyedan, M.H. Enayati, M. Hashempour, A. Vicenzo, M. Bestetti, Synthesis and characterization of sol-gel derived non-stoichiometric aluminum phosphate coating, Surface and Coatings Technology, 351 (2018) 128-135.

[30] Bio-Rad Laboratories, Inc. SpectraBase, Free Spectral Database.

[31] W.J. Bruckard, J.T. Woodcock, Characterisation and treatment of Australian salt cakes by aqueous leaching, Minerals Engineering, 20 (2007) 1376-1390.

[32] C. Balasubramanian, S. Bellucci, G. Cinque, A. Marcelli, M.C. Guidi, M. Piccinini, A. Popov, A. Soldatov, P. Onorato, Characterization of aluminium nitride nanostructures by XANES and FTIR spectroscopies with synchrotron radiation, Journal of Physics: Condensed Matter, 18 (2006) S2095-S2104.

[33] M. Mahinroosta, A. Allahverdi, Enhanced alumina recovery from secondary aluminum dross for high purity nanostructured γ-alumina powder production: Kinetic study, Journal of Environmental Management, 212 (2018) 278-291.

[34] A. Meshram, K.K. Singh, Recovery of valuable products from hazardous aluminum dross: A review, Resources, Conservation and Recycling, 130 (2018) 95-108.

[35] O. Manfredi, W. Wuth, I. Bohlinger, Characterizing the physical and chemical properties of aluminum dross, JOM, 49 (1997) 48-51.

[36] G.A. Slack, T.F. McNelly, Growth of high purity AlN crystals, Journal of Crystal Growth, 34 (1976) 263-279.

[37] B. Zhou, Y. Yang, M. Reuter, Process modeling of aluminum scraps melting in molten salt and metal bath in a rotary furnace, Light Metals, (2004) 919-924.

[38] D.G. Graczyk, A.M. Essling, E.A. Huff, F.P. Smith, C.T. Snyder, Analytical chemistry of aluminum salt cake, Light Metals, (1997) 1135-1140.

[39] R.D. Peterson, L. Newton, Review of aluminum dross processing, in Light Metals: Proceedings of Sessions, Light Metals, (2002) 1029-1037.

[40] Q. Li, Q. Yang, G. Zhang, Q. Shi, Investigations on the hydrolysis behavior of AlN in the leaching process of secondary aluminum dross, Hydrometallurgy, 182 (2018) 121-127.

[41] P. Li, J. Wang, X. Zhang, X. Hou, B. Yan, H. Guo, S. Seetharaman, Molten salt-enhanced production of hydrogen by using skimmed hot dross from aluminum remelting at high temperature, International Journal of Hydrogen Energy, 42 (2017) 12956-12966.

[42] E. David, J. Kopac, The Assessment of the Recycling Process of Aluminum Hazardous Waste and a New Route of Development, Materials Today: Proceedings, 10 (2019) 340-347.